Morphology of titania coatings on silica gel

Aree Hanprasopwattana [a], Thomas Rieker [b], Allen G. Sault [c] and Abhaya K. Datye [b,*]

Center for Microengineered Materials and Departments of Chemistry [a] and Chemical and Nuclear Engineering [b], University of New Mexico, Albuquerque, NM 87131 USA
E-mail: datye@nm.edu
[c] Sandia National Laboratories, Catalysis and Chemical Technologies Department, NM 87185-0710, USA

Received 11 February 1997; accepted 19 March 1997

Control of the hydrolysis and condensation of soluble precursors of titanium is shown to yield oxide coatings of well-defined morphology. A "smooth" coating, consisting of patches of titania on silica, causes only a small increase in the surface area, from 130 m^2/g for the uncoated silica gel to 154 m^2/g. On the other hand, the "rough" coating, which consists of 3 nm diameter titania particles dispersed over the silica surface, results in an increase in the BET surface area to 350 m^2/g. The specific titania surface area was determined via isopropanol dehydration activity and was found to be comparable to the BET surface area indicating that the titania phase is responsible for the increase in surface area. Small angle X-ray scattering (SAXS) and transmission electron microscopy (TEM) provide definitive evidence for the coating morphology while X-ray photoelectron spectroscopy (XPS) was used to determine the dispersion of the titania. The supported titania maintains its surface area upon calcination at temperatures up to 873 K while unsupported titania looses much of its surface area. Also demonstrated in this work is a novel preparation method using titanium bis-ammonium lactato dihydroxide (TALH), a water soluble precursor.

Keywords: preparation of titania/silica, isopropanol dehydration as a probe of titania/silica, transmission electron microscopy of titania/silica, small angle X-ray scattering of titania/silica, thermal stability of supported titania, nanostructured titania/silica

1. Introduction

Titania is a technologically important material, both as a catalyst [1] and a support [2]. Titania in high surface area form has low mechanical strength, limited extrudability and, importantly, low thermal stability. Therefore, effort has been devoted in recent years to coat titania onto high surface area supports such as silica and alumina to improve the thermal stability of the surface area of titania.

In previous work, we deposited [3] a monolayer of titania on silica to alter the surface chemistry [4] and improve the coating of boron nitride thin films on the silica [5]. The common feature of these studies was the use of non-porous Stöber silica spheres [6] as substrate, which allowed the nature of the coating to be determined by transmission electron microscopy (TEM). The reactivity for propene formation during 2-propanol dehydration shows a linear correspondence with Brunauer–Emmett–Teller (BET) surface areas of titania powders ranging from 35 to 235 m^2/g [7], indicating that propene formation activity can be used as a measure of titania surface area in titania-coated silica. Such estimation of titania surface area is possible because the reactivity of titania for 2-propanol is greater than that of silica by at least two orders of magnitude. We have previously shown that alcohol dehydration activity can also be used to measure the surface area of titania in titania/silica thin films [8].

The control of titania morphology in thin films is important since it provides a tool to microengineer a catalyst surface, as shown in our recent work on hydrotreating catalysts [9]. In that work, it was found that the activity of MoS_2 on microroughened titania on silica spheres was over an order of magnitude greater than that of the MoS_2 supported on bulk titania. In the present study, we have extended our work on non-porous silica spheres (12 m^2/g) to higher surface area silica gels. Two precursors, titanium butoxide (TBOT) and titanium bis-ammonium lactato dihydroxy complex (TALH) were used in this study. By varying the hydrolysis and condensation reactions of these precursors, we can form molecular clusters, colloidal particles or second-phase titania precipitates, as shown schematically in figure 1.

Among the different characterization techniques used, X-ray fluorescence (XRF) and BET can give information about the bulk weight loading and the total surface area of the sample. 2-propanol dehydration can tell us about the specific surface area of the titania, but provides no information on titania morphology. For example, a high surface area of titania measured by alcohol dehydration could arise due to particle surface roughness, porosity of the titania or the presence of small primary particles of titania. Such information can be derived from transmission electron microscopy (TEM). However, TEM has the following limitations: the sample must be thin enough to be electron transparent and the

* To whom correspondence should be addressed.

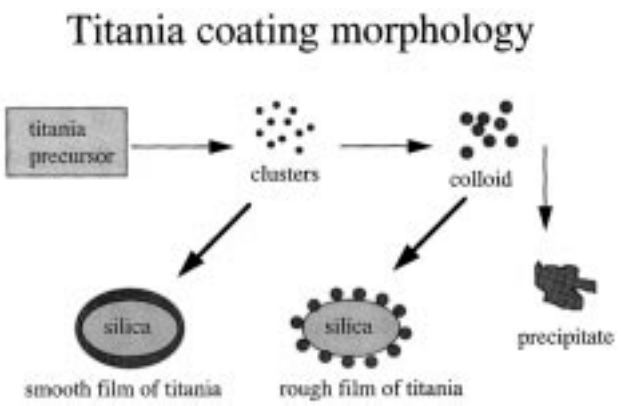

Figure 1. Schematic representation of titania deposition routes that can lead to a "smooth" coating, a "rough" coating, or precipitation as a second phase.

sample should not charge excessively during electron exposure. These requirements restrict the application of high resolution TEM to the external surfaces of the oxide support, with a typical micrograph showing a region that is 50 nm × 50 nm on a side. Hence, the morphology of the titania coating in the interior of the support cannot be studied by TEM. For this purpose, we have used the technique of small angle X-ray scattering (SAXS).

Small angle X-ray scattering arises from inhomogeneities in the electron density within a material. Inhomogeneities coherently scatter radiation in the forward direction. The intensity distribution as a function of angle is dependent on the shape, size, concentration and interfacial roughness of the inhomogeneities [10]. Hence, the technique is useful for the study of particles as well as voids. SAXS is particularly useful for elucidating the macroscopic structure (volume sampled ranges from ~ 0.02 to 1 mm^3) of amorphous heterogeneous materials on length scales ranging from tens of angstroms to a few tenths of a micron. This range of length scales is difficult to cover by other characterization techniques. SAXS has been used extensively to understand the formation mechanism of silica and titania gels because it can give information about the distribution of electron density and mass in the primary particle [11–13]. However, SAXS either alone or with other methods has not been applied to study coating formation and morphology.

When depositing titania on a high surface area silica, it is important to know if the titania deposits preferentially on the outer surface of the oxide support particles. In recent work reported in the literature, this question has been addressed using a variety of techniques: X-ray photoelectron spectroscopy (XPS) [14], scanning electron microscopy (SEM) and energy dispersive spectroscopy (EDS) [15] as well as electron microprobe analysis [16]. While XPS yields the dispersion of the titania on silica, there is no information on the morphology of the coating, particularly within the internal pore structure of the oxide support. Similarly, SEM and electron probe analysis show the distribution of the titania on a submicron scale, but without any understanding of the nanoscale morphology of the oxide coating. As we show in this paper, the combination of SAXS, high resolution TEM and XPS provides unique insight into the nature of dispersed oxide coatings.

A review of previous work [16] shows that precipitation ($TiCl_4$ and NH_4OH) and impregnation (Ti-isopropoxide in alcohol) both give a higher concentration of titania at the outer surface of the silica particles. Only grafting [16,17] (reaction of the surface hydroxyls with the precursor) provides a uniform concentration of titania [14,3]. However, the titania loading achieved via grafting is typically less than a monolayer, and involves the use of air-sensitive precursors and solvents, which limit industrial application of this method. Therefore, this study has explored a novel approach for depositing the titania on the silica. The precursor titanium bis-ammonium lactato di- hydroxide (TALH) is water soluble and can be hydrolyzed with urea at 363 K. Hydrolysis is initiated by heating after the pores are filled with the reactants. By controlling the concentrations of the reagents, we are able to control the morphology from that of a smooth coating of titania to a nanocrystalline deposit. The surface area of the silica increases after deposition of the titania and, as shown in this paper, the higher surface area is preserved at temperatures up to 923 K. The nature of titania coatings obtained with a butoxide precursor is compared with those obtained from TALH.

2. Experimental

2.1. Sample preparation

The silica used in this study was a mesoporous Norton silica gel (sample number 9316080) with a median pore diameter of 240 Å and a measured BET surface area of 130 m^2/g. The silica extrudates were ground in a mortar and pestle before use. Commercial silicas must be treated to remove sodium introduced during preparation since sodium inhibits alcohol dehydration. To remove the sodium, 6 g of silica was dispersed in 30 ml of 1 part HNO_3 to 2 parts H_2O. The mixture was stirred and heated to about 333 K for 1 h. The mixture was subsequently diluted with 50 ml of deionized water, filtered and washed with seven, 20 ml aliquots of deionized water. Finally the silica was dried in air at 383 K.

For the titanium butoxide (TBOT) coatings, one gram of the acid-washed silica was dispersed in a mixture of 1.5 ml water, 250 ml ethanol, and 1 ml of TBOT. This silica dispersed mixture was then refluxed at 351 K for 20 h. The mixture was filtered and washed four times with 20 ml aliquots of ethanol. For the titanium bis-ammonium lactato dihydroxide (TALH) precursor, the first step was the preparation of an aqueous mixture of

the TALH precursor, urea and silica. The aqueous mixture was prepared as follows: 6.1 ml of 50% aqueous solution of TALH was added to 200 ml deionized water. Next, 1 g of the silica gel and 6.9 g of urea were added to this solution. This mixture was stirred at room temperature for 1 h and refluxed at 373 K for 20 h. The coated silica gel was then separated by centrifuging the mixture. The excess titanium precursor was then removed from the coated sample by washing with hot deionized water three times. The washed (titania-coated) silica gel was then dried in air at 383 K for 8 h.

2.2. Characterization

The sodium content of the samples was determined by atomic absorption spectroscopy (AA). The loading of titania on silica gel was analyzed by energy dispersive X-ray spectroscopy (EDS) and X-ray fluorescence (XRF). Electron microscopy was performed on a Jeol 2010 microscope equipped with an Oxford instruments EDS system with a Link thin window detector. SAXS was performed at the University of New Mexico/Sandia National Laboratories/University of Missouri joint Small-angle Scattering Laboratory (http://saxs-comm.unm.edu). The wide q-range SAXS data presented here is obtained by combining data collected on the Bonse-Hart spectrometer and the pinhole instrument (short geometry). SAXS samples were prepared by trapping sample powders inside a thin washer with self-adhesive tape windows. This produced samples of net thickness ranging from 0.03 to 0.1 mm.

X-ray photoelectron spectroscopy (XPS) measurements were made in a combined ultra-high vacuum surface analysis/atmospheric pressure reactor system. All spectra were taken using a VG Microtech CLAM2 hemispherical analyzer operated at a pass energy of 50 eV and a slit width of 4 mm, corresponding to an analyzer resolution of 1.0 eV. A Mg Kα X-ray source oriented 50° away from the analyzer lens axis provided primary excitation. Ti 2p/Si 2p intensity ratios were determined by integration of the respective peak areas after subtraction of a linear background.

2.3. Alcohol dehydration as a test for titania specific surface area

The effective titania surface area of the coatings on silica gel were measured using the reactivity for 2-propanol dehydration. A series of titania samples with surface areas ranging from 40 to 230 m^2/g was synthesized using the method suggested by Nishiwaki et al. [18] and used for reactivity measurements. 30 mg of sample was loaded in a quartz U-tube. For the dehydration activity measurements, 2-propanol was introduced into a 20.2 sccm stream of flowing helium using a saturator at room temperature. Dehydration activity was measured between temperatures of 448 and 648 K after initial pretreatment in He at 773 K. The propene formation activity varied linearly with titania BET surface area and the activity was found to be independent of the pretreatment temperature, up to a pretreatment temperature of 773 K. The calibration curve for determining titania surface area is shown in figure 3 of our previous work [7]. The specific titania reactivity is 3.24×10^{-8} moles of propene formed/($s\,m^2$) at 523 K.

Since this correlation was obtained with anatase titania, it is necessary to pretreat the titania coatings to 773 K to ensure that crystallization is complete. The above mentioned correlation works well with the TBOT precursor but not with the TALH precursor since helium treatment for 8 h at 773 K may not completely remove all the organic groups. Hence a new calibration was prepared for samples prepared from this precursor yielding a specific reactivity of 1.31×10^{-8} moles of propene formed/($s\,m^2$) at 523 K.

3. Results and discussion

3.1. Titania precursor chemistry

In this paper, we describe two differing morphologies of titania coatings that can be obtained on the silica gel. The method involves the hydrolysis and condensation reactions of a soluble titanium precursor. If the precursor is allowed to hydrolyze and condense only to the extent of forming oligomeric clusters which are then allowed to nucleate on the surface of the support, smooth coatings will be formed. If the precursor is allowed to hydrolyze and condense till colloidal sized particles are formed as shown in figure 1, a rougher coating will result. If the hydrolysis–condensation proceeds very fast, precipitation of titania would be expected. We find that, with either precursor, the nature of coatings obtained depends upon the titania loading, which in turn is determined by the amount and concentration of reagents, deposition temperature and time of reaction. The titania coating chemistry is shown in scheme 1.

With the titanium alkoxide precursor, dilute solutions of the reactants, i.e. water (hydroxyl group precursor) and alkoxide (titanium precursor) in excess ethanol allow physical separation of the reactants. Once the mixture containing the silica is refluxed, the high temperature and mobility of the reacting species allow the orderly precipitation of titania containing polymeric species onto the silica. However, titanium butoxide is an extremely water-sensitive precursor. Therefore, the maximum titania loading that can be achieved without second-phase precipitation of titania is limited. In general, as the loading of the dispersed phase is increased we see precipitation of a second phase in addition to a coating on the support.

An ideal precursor would be one that is soluble in water and hydrolyzes slowly. The hydrolysis procedure

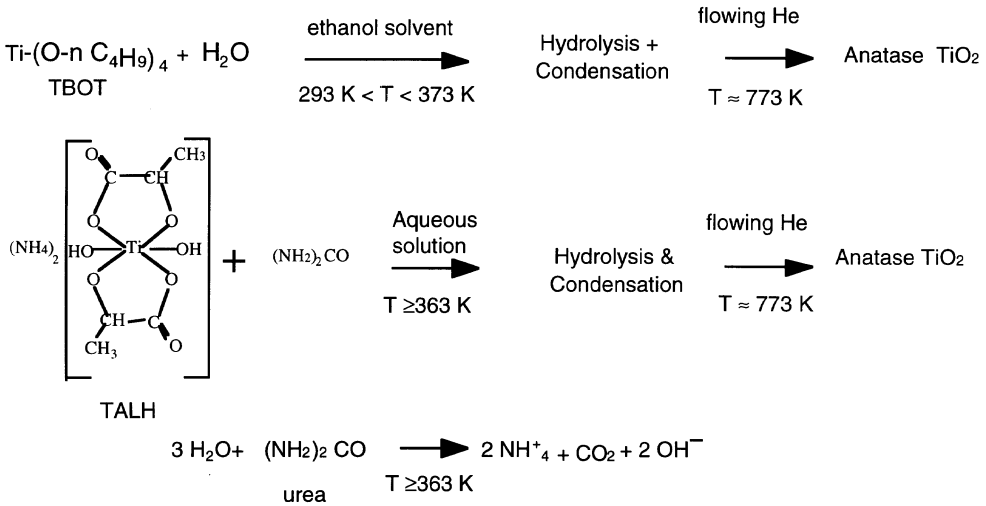

Scheme 1.

should preferably include a delayed OH group production after the pores of a silica are already filled with the titanium precursor and the reagent that induces the hydrolysis and condensation. Thus, we want a retarded–delayed hydrolysis. The choice of a delayed OH group producer dictates the use of urea, which satisfies the requirements for this reaction. Urea hydrolyzes extremely slowly at room temperature but more rapidly at 363 K. Therefore, with a water-soluble titanium precursor and urea, we can first fill the pores with the titanium precursor and then hydrolyze it inside the pores. The precursor that fulfills the above properties is titanium bis-ammonium lactato dihydroxide (TALH). This molecule dissolves in water but does not hydrolyze under ambient conditions. Therefore, this slowly hydrolyzing chelate compound can be hydrolyzed inside the pores at higher temperature with the OH groups provided by urea.

Table 1 shows the samples that were prepared in the course of this study. The Norton silica gel has a surface area of 130 m^2/g and its surface area increases after coating with either precursor, TBOT or TALH. The difference is in the magnitude of the increase, with TiO_2/SiO_2 (TBOT) sample showing only an increase to 154 m^2/g while the TiO_2/SiO_2 (TALH) shows an enormous increase to 350 m^2/g. The titania loadings are also different, with the TBOT sample having a loading of 18.1 wt% and the TALH sample having a loading of 46.2 wt% titania. In both these samples, the effective titania surface area agrees with the BET surface area, suggesting coverage of the silica by the titania. The difference in titania loading between the two samples is caused by the higher concentrations of precursor used in the case of the TALH precursor. With lower concentrations of the TALH precursor, it is possible to obtain coatings similar to those achieved with the TBOT precursor.

3.2. Characterization of the titania/silica by TEM, SAXS and XPS

3.2.1. Uncoated silica gel

Figures 2a and 2b show electron micrographs of the silica gel as-received. Primary particles can be seen that

Table 1
Surface area and titania loading of the samples investigated

Name	BET [a] (m^2/g)	Alcohol dehydration activity of TiO_2 (mol propene/(g s))$\times 10^6$ at 523 K	Effective TiO_2 surface area from alcohol dehydration [b] (m^2/g)	TiO_2 loading (%wt from XRF)
silica gel	130	3×10^{-3}	–	–
bulk TiO_2 (TALH)	168	2.2	168	–
TiO_2/SiO_2 (TBOT)	154	4.6	142	18.1
TiO_2/SiO_2 (TALH)	350	4.8	366	46.2

[a] The BET surface area is quoted for a sample pretreated at 773 K. The 773 K pretreatment is necessary to use the isopropanol dehydration activity as a measure of the titania surface area.

[b] As stated in the text, the correlation between surface area and isopropanol dehydration activity differs for the two precursors. The difference is dictated by the inability of the 773 K pretreatment in helium to remove all the organic groups from the TALH precursor, causing its specific activity to be lower than that of coatings derived from the TBOT precursor.

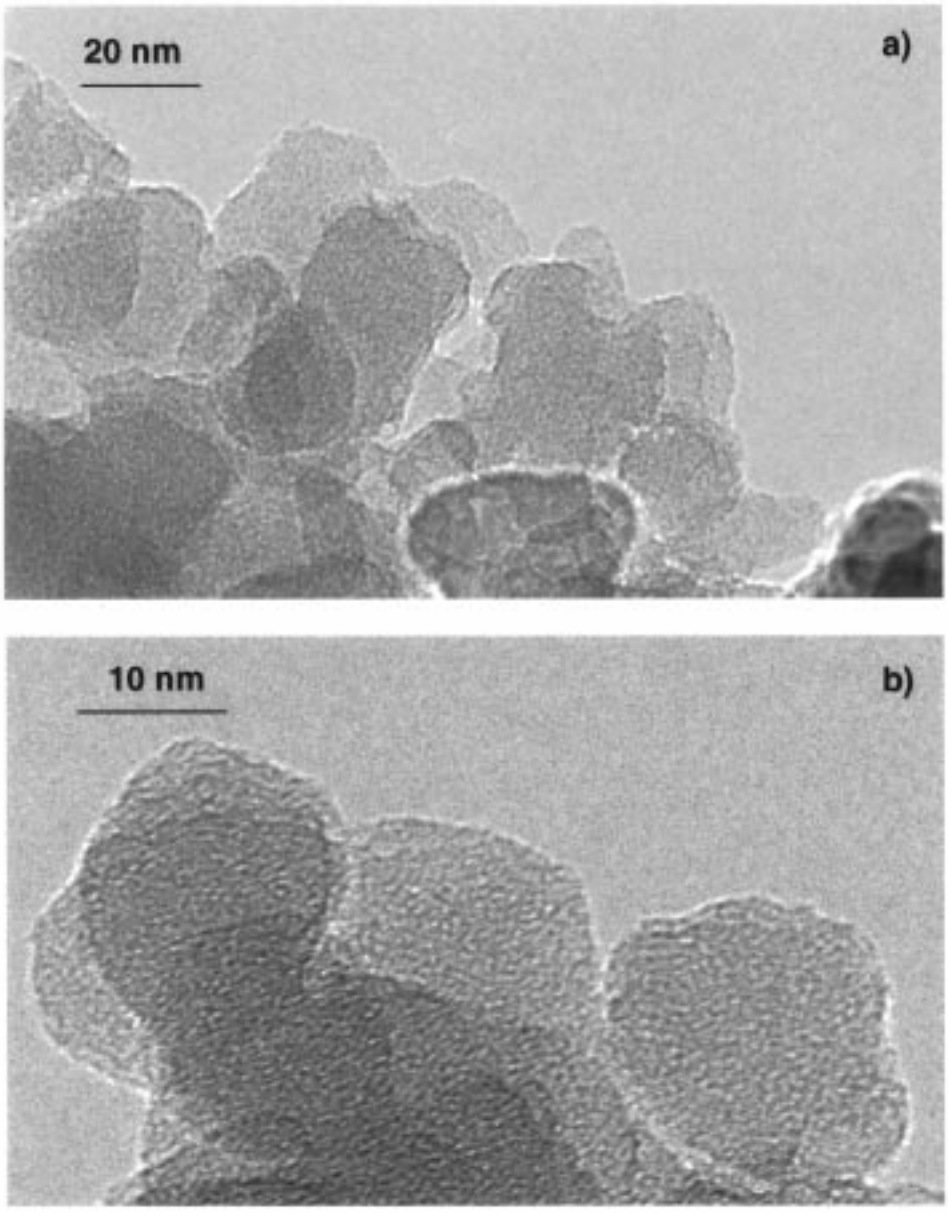

Figure 2. TEM images of uncoated Norton silica gel. (a) Low magnification view shows the primary silica particles and (b) higher magnification view showing the characteristic contrast from the amorphous silica and the nature of the silica surface.

range in diameter from 15 to 30 nm. The higher magnification view shows contrast characteristic of an amorphous structure. The primary particles are non-porous as evident from the BET surface area which is consistent with an average spherical particle diameter of 18.2 nm using the equation $S = 6/\rho d_p$ where ρ is density and d_p is particle diameter. The SAXS data for the uncoated silica gel is presented in figure 3.

The SAXS data is analyzed using the unified approach [19] in which the SAXS curve is divided into multiple structural levels. Each level corresponds to a particular feature size manifest by a shoulder (Guinier region) in log–log plots of $I(q)$ vs. q, which tapers on the high q side to a power law region, $I(q) \sim q^{-\alpha}$. The scattering vector q is defined by $q = (4\pi/\lambda)\sin(2\theta/2)$ and 2θ is the scattering angle. Fits to the shoulder region using the Guinier approximation $I(q) \sim \exp(-q^2R_g^2/3)$ yield the characteristic size of the scatterer, called the radius of gyration R_g. The radius of gyration is a center of mass-like quantity, averaged over the sample volume. For simplicity, we assume all features in the samples are spherical in shape and give dimensions here and in the figures as real space diameters, with the conversion $d = 2\sqrt{\frac{5}{3}}R_g$. The power law region describes the mass-fractal ($-3 < \alpha < -2$) or surface-fractal ($-4 < \alpha < -3$) scaling of the scatterer [20]. Power law values of $\alpha = -4.0$ indicate a sharp, smooth interface between two regions of different electron density. Structural models are built

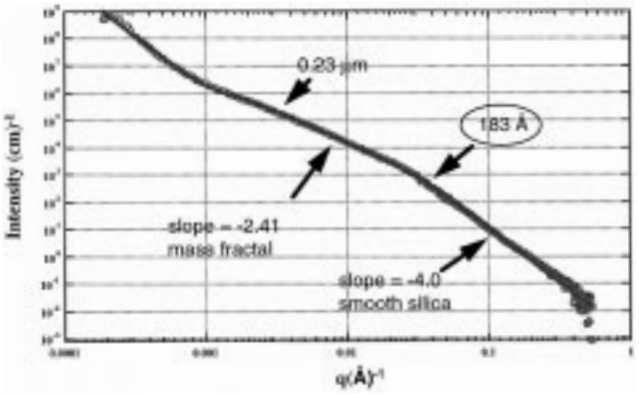

Figure 3. SAXS data for silica gel (○) and fit (——), plotted as absolute intensity vs. wave vector q. Power law regions, $I(q) \sim q^{-\alpha}$, are seen as straight lines in the log–log plot. The primary silica particle is inferred to be ~ 180 Å in diameter. These particles form 0.23 μm diameter diffusion-limited aggregates, as shown figure 4.

from the smallest feature size or high q shoulder in the SAXS curve (first structural level) progressing to larger feature sizes, or shoulders at lower q.

The SAXS curve for the silica gel, figure 3, shows the primary silica particle to be approximately 180 Å in diameter (shoulder around $q = 0.03$ Å^{-1}) and to have an abrupt SiO_2 vacuum interface, as evidenced by the power law slope of -4. The BET surface area is 130 m^2/g which is consistent with the primary particle size of 182 Å. SAXS provides additional information on the meso-scale structure. The primary silica particles aggregate to form a 0.23 μm diffusion-limited aggregate (power law slope -2.5) [21] as determined from the low q shoulder in the SAXS data (around $q = 0.0025$ Å^{-1}). Figure 4 shows a low magnification view of a typical silica grain in this sample. The aggregation of the primary silica particles can be seen in this image. The size of these aggregates varies from 0.1 μm all the way to greater than 1 μm. Since the shoulder in the SAXS is not very well defined, there is greater uncertainty about the size of this diffusion-limited aggregate, as measured by SAXS, compared to the size of the primary silica particle where the inflexion in the scattering curve is much more pronounced.

3.2.2. TBOT-coated silica gel

Figures 5a and 5b show electron micrographs of the sample coated with the TBOT precursor. Figure 5a, which is a low magnification view, shows that the tita-

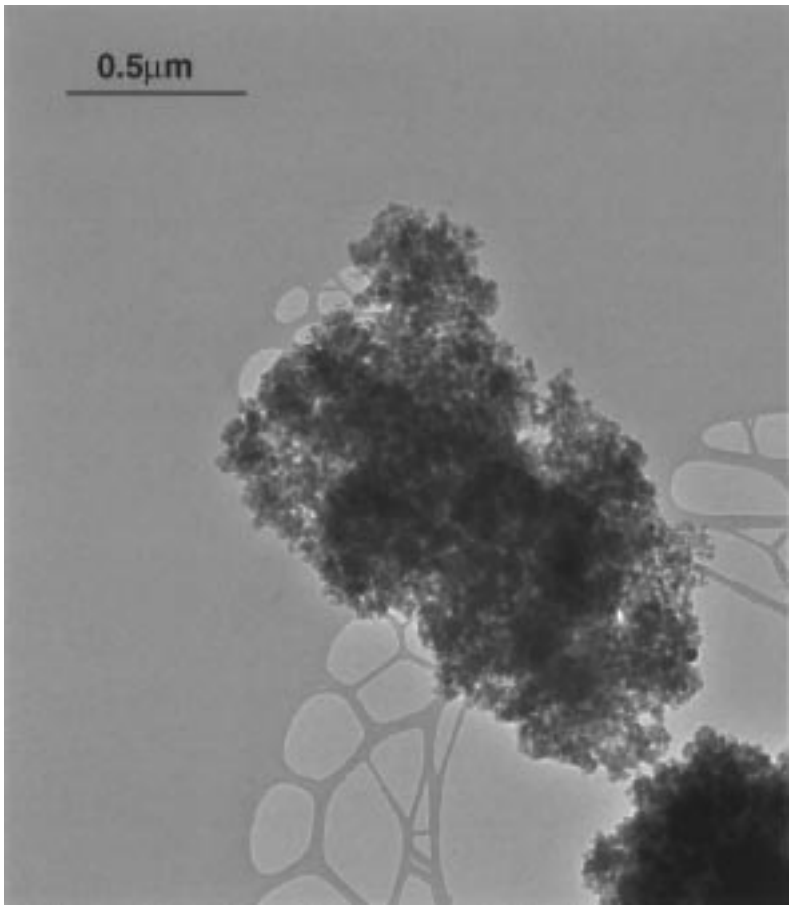

Figure 4. Low magnification TEM image of the commercial silica gel, showing the micron-sized porous silica aggregates. The pore volume in this silica is essentially the void space between the primary particles seen in figure 2a.

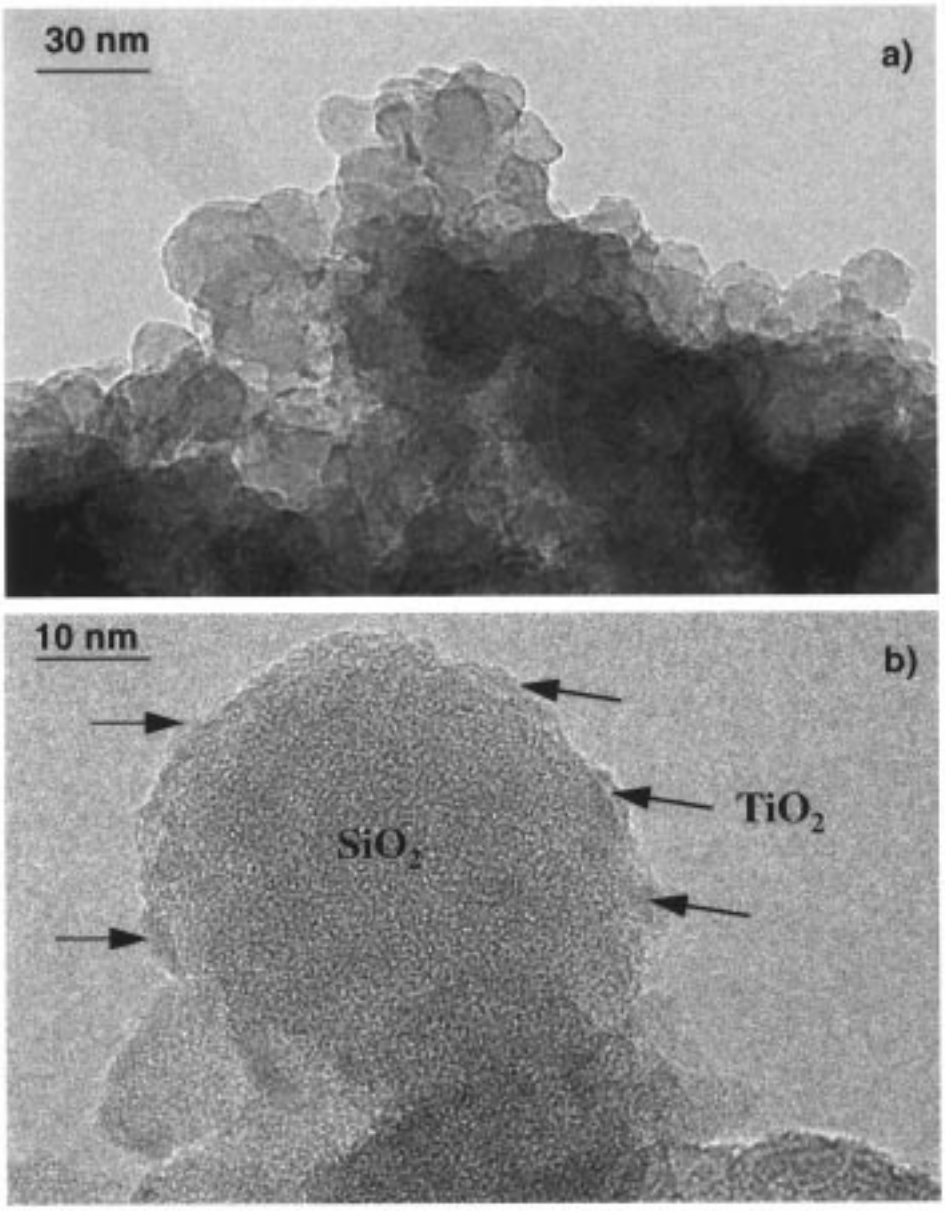

Figure 5. TEM images of the titania-coated silica using the TBOT precursor. (a) Low magnification view shows sample morphology very similar to that of the uncoated silica, no second-phase titania particles are seen. (b) The arrowed patches exhibit contrast different from that of the bare silica and represent the only observable evidence of the titania coating. The presence of the titania is also confirmed by elemental analysis using energy dispersive spectroscopy.

nia-coated silica looks very similar to the uncoated silica seen in figure 2a. No second-phase precipitates of titania were seen in the TEM. A higher magnification image of one of the silica particles is shown in figure 5b. The presence of the titania is evident in the patches indicated by arrows that exhibit very different contrast from the underlying silica support (cf. figure 2). Elemental analysis in the TEM also shows that the titania is well dispersed. Since the titania is present in patches as shown in figure 5b, the overall morphology of the coating is quite smooth and there is only a minimal surface area increase i.e. from 130 to 154 m^2/g.

As with the TEM images, the presence of the titania is evident in the X-ray scattering data. For the titanium butoxide-coated silica, the smallest feature size seen in the SAXS data (figure 6) is approximately 210 Å in diameter. While this size is greater than that for the uncoated silica gel, what is more striking is the slope of the scattering curve in the high q region. In contrast to the uncoated silica (power law exponent of -4.0), the slope has changed to a power law exponent of -3. The lower slope would suggest a surface fractal produced by the irregular titania coating of the silica particles. This is consistent with the TEM images in figure 5. There is no evidence of colloidal titania particles on the microscopic scale (TEM) or on a macroscopic scale (SAXS). The low q

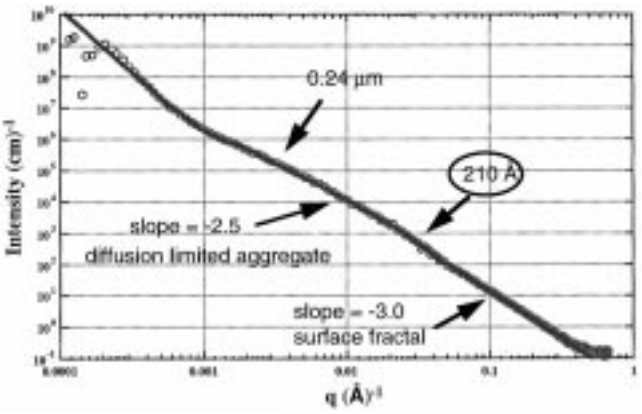

Figure 6. SAXS data (○) and fit (——) for titania-coated silica using the TBOT precursor. The primary particle is now a surface fractal of titania-coated silica approximately 210 Å in size. These particles form a 0.24 μm diameter diffusion-limited aggregate.

region of the SAXS curve indicates the formation of a 0.24 μm diffusion-limited aggregate which is comparable in size to the uncoated silica gel.

For this sample, an XPS Ti 2p/Si 2p intensity ratio of 2.6 is obtained for the fresh sample, falling to 2.4 after treatment in Ar at 773 K for 4 h. Based on the method of Kerkhof and Moulijn [22] for calculating XPS intensity ratios for coatings on high surface area materials, but assuming an average photoelectron takeoff angle of 57.3° as recommended by Frydman et al. [23], and using reported attenuation lengths (AL) [24] and sensitivity factors [25] (corrected for differences in atomic density and AL between the elements and the oxides), the measured peak area ratios are found to correspond to a titania coating thickness of 0.3–0.4 nm. This result is in excellent agreement with the coating thickness calculated from the SiO_2 surface area and the known titania loading (18%) if a uniform titania overlayer is assumed. This agreement, coupled with the absence of many observable titania particles in TEM, demonstrates conclusively that the titania is uniformly dispersed on the silica substrate with little or no second-phase titania particle formation. The very minor change in the Ti 2p/Si 2p ratio with heat treatment indicates that no significant sintering of agglomeration of the titania phase occurs during pretreatment of the sample.

3.2.3. TALH-coated silica gel

Figures 7a and 7b show electron micrographs of the sample coated with TALH precursor. In the low magnification view (figure 7a) the presence of small black dots is indicated by arrows. Such features were not seen in the uncoated silica (figure 2) or the TBOT-coated silica (figure 5). These dots are colloidal titania particles of about 3 nm in diameter deposited on the silica surface. When examined at higher magnification, these dots show up as particles of crystalline titania with lattice fringes consistent with the anatase phase. It is possible, however, that the crystallization could have occurred under the action of electron beam. In addition to these nanometer-sized titania islands, we also see regions where the titania concentration is very high. Closer examination in the TEM reveals these to be aggregates of titania particles similar to those shown in figure 7b deposited on the silica.

The SAXS data for this sample (figure 8) shows that the smallest feature is associated with the primary particles having a diameter of $\sim$ 29 Å and smooth surface (power law exponent of -4). As seen in the TEM images, these are the primary particles of titania. Since the titania particles are deposited on the silica, we would expect to see a feature that corresponds to the primary silica particles. Indeed, as seen in figure 8, we see particles with a mean diameter of 205 Å whose surface must be a mass fractal (power law slope -2.76). The next larger feature is a 0.41 μm diffusion-limited aggregate, which represents aggregates of the titania-coated silica particles. Each of the features seen in the SAXS is consistent with the TEM observations reported in figure 7. However, the number density of the titania particles seen by TEM does not agree with the number density one would expect based on the overall titania loading as determined by XRF. A similar discrepancy is seen by XPS.

Given the substantially higher titania content of the sample prepared from the TALH precursor, a higher Ti 2p/Si 2p intensity ratio is expected for this sample. Experimentally, however, the measured ratio is found to be 1.4, lower than that from the TBOT sample. A calculation of the expected XPS ratio based on bulk analysis of titania content and TEM images showing the presence of 3 nm titania particles, predicts an XPS ratio of 8.0. Furthermore, the calculations also indicate that to achieve a titania loading of 46 wt% through coverage of the silica by 3 nm particles, more than half of the silica surface would have to be covered by titania particles. Not only is this level of coverage not apparent in the TEM images, but EDS results indicate a titania loading of only 15 wt% on the silica particles. Calculation of the expected XPS ratio based on this loading and the assumption that all titania is present as 3 nm particles results in a Ti/Si ratio of 0.90, reasonably close to the experimental value of 1.4. Furthermore, this lower loading corresponds to coverage of only 10–12% of the silica surface by the 3 nm titania particles, a result much more consistent with the TEM images.

In order to reconcile the above discrepancies in the available data, the presence of a second, bulk titania phase must be invoked. Indeed, TEM images occasionally show second-phase particles that are titania rich as seen by EDS. This second phase could make a substantial contribution to the overall titania content and result in the bulk value of 46 wt% titania, even though the titania content on the silica phase is relatively small. The presence of these particles would also increase the measured Ti 2p/Si 2p ratio over that calculated from EDS

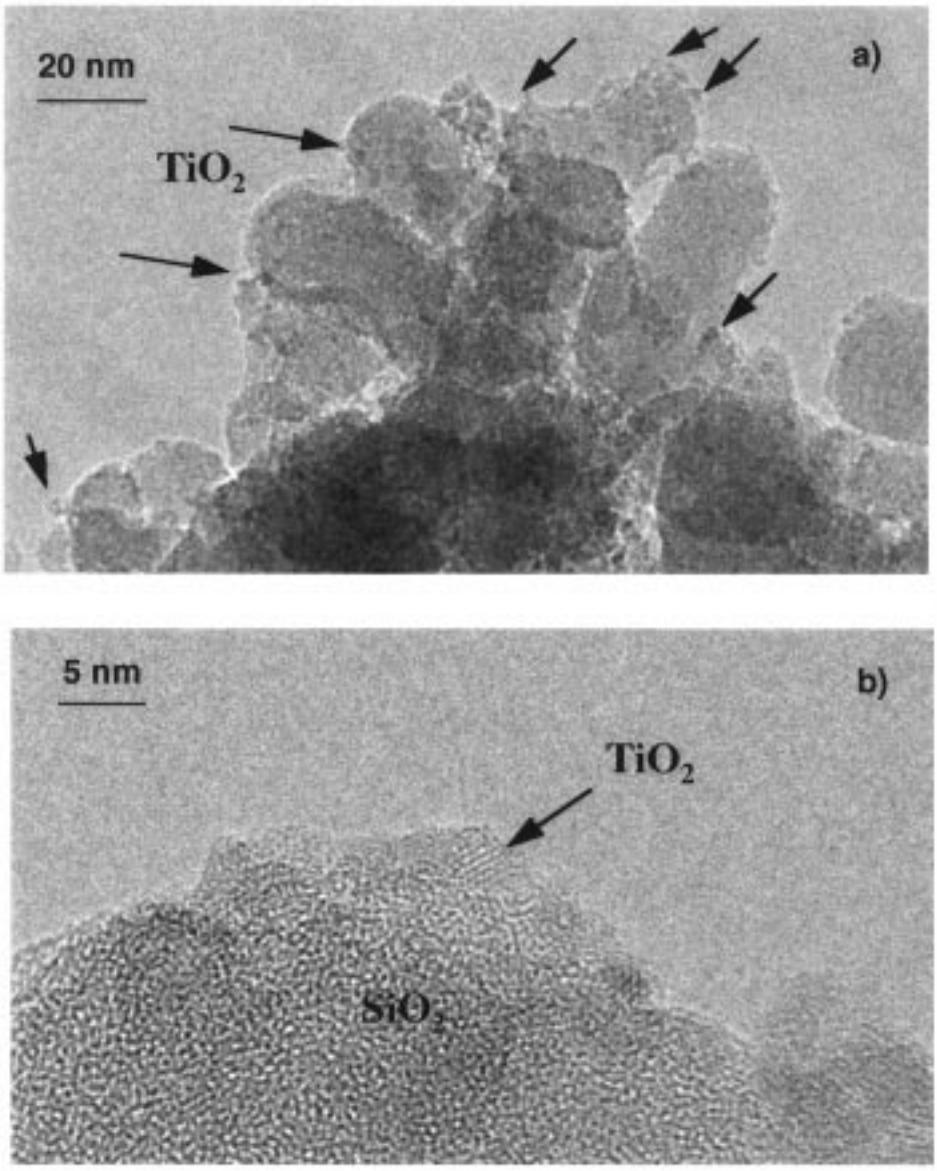

Figure 7. TEM images of the titania-coated silica using the TALH precursor. (a) The low magnification view shows small black dots decorating the silica surface. (b) At higher magnification, these black dots show up as discrete particles of titania. Since these particles are randomly oriented, in any micrograph only a few of these particles exhibit well defined lattice fringes.

data for the silica phase alone, and could easily make up the difference between the calculated and measured values.

3.3. Titania coating surface area and thermal stability

The morphology of the titania coating significantly affects the surface area of the titania/silica sample. In the case of the TBOT-derived coating (18 wt%), the increase in surface area is modest, from 130 to 154 m^2/g. The increase in surface area can be associated with the roughening of the silica surface caused by patches of titania, as seen in figure 5b. With the TALH precursor, we have a higher titania loading (46 wt%) and the surface area increases to 350 m^2/g. The titania is present in the form of 3 nm particles on the silica as well as in the form of second-phase aggregates of 3 nm titania particles. The presence of this second phase has a large effect on measured surface areas. The surface area of the silica phase would remain at or near 130 m^2/g, so the surface area of the second-phase titania particles would have to be very large. In a 1 g sample, 0.54 g of silica would be present and contribute ~ 70 m^2 to the total surface area. The remaining 280 m^2 would have to be associated with the titania phase, which would contain most of the 0.46 g of titania in the sample. In this scenario, the surface area of the second-phase titania would therefore be 280 $m^2/0.46\ g = 610\ m^2/g$. TEM images show that the second-phase particles are composed of agglomerates of small titania particles. Based on the bulk density of anatase

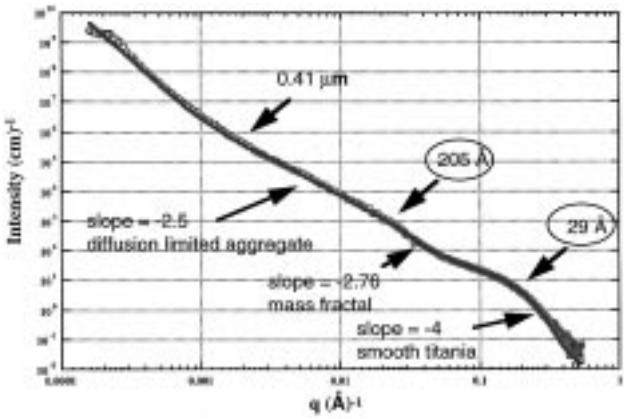

Figure 8. SAXS data (○) and fit (——) for the titania-coated silica using the TALH precursor. The smallest feature corresponds to particles ~ 29 Å in diameter. This is known to be colloidal titania from TEM, see figure 7. The colloidal titania and the primary particles from the silica gel form a mass-fractal structure ~ 205 Å in size. The titania-coated silica particles form diffusion-limited aggregates approximately 0.41 μm in diameter.

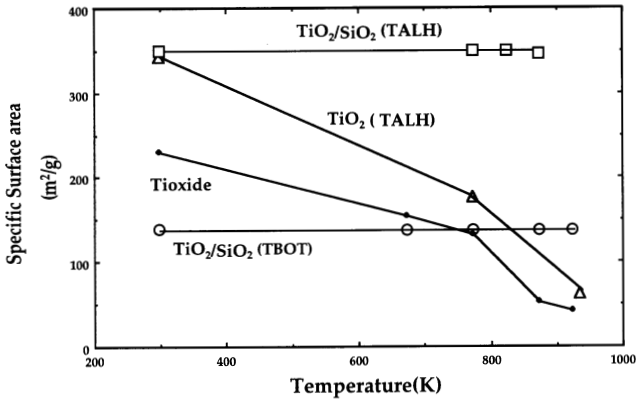

Figure 9. Thermal stability plot of TiO_2 on SiO_2 samples compared with a commercial TiO_2 (Tioxide) and bulk TiO_2 (TALH).

(3.89 g/cm^3), we can estimate the required average particle diameter to be 2.5 nm, in reasonable agreement with the 3 nm particle diameter derived from TEM and SAXS.

Since the silica phase is only partially covered by titania particles, it would be expected that the total BET surface area of the samples should be slightly higher than the titania surface area determined by alcohol dehydration. The apparent equality of the two surface area measurements is most likely due to small errors in calibration of the alcohol dehydration measurement. Since upwards of 80% of the surface area is contributed by the second-phase titania, it would take only a small error to result in a spuriously high value for the titania surface area and give rise to the apparent agreement, even though some bare silica surface is present.

Figure 9 shows the higher thermal stability of the two titania-coated silicas compared to commercial TiO_2 (Tioxide) and unsupported TiO_2 prepared from the TALH precursor. The surface area of TiO_2/SiO_2 (TALH) and of TiO_2/SiO_2 (TBOT) remained almost the same after calcination at temperatures up to 873 K for TiO_2/SiO_2 (TALH) and up to 923 K for TiO_2/SiO_2 (TBOT). In contrast, the surface area of unsupported TiO_2 (TALH) as-prepared is 342 m^2/g but decreases to 57 m^2/g after calcination at 933 K. A similar decrease in surface area is seen for a commercial TiO_2 (Tioxide) which dropped from a surface area of 234 m^2/g as-received to 46 m^2/g after calcination at 923 K. The thermal stability of the TALH-coated silica is remarkable in view of the large contribution to the surface area from a second-phase titania. However, we found in the TEM that the second-phase titania particles were always associated with the silica phase. Therefore, we suspect that the silica support helps to stabilize not only the individual titania particles but also the aggregates of titania particles against sintering and loss of surface area.

4. Conclusions

Titania coatings of differing morphology were prepared by controlling the hydrolysis and condensation of soluble titanium precursors. The two precursors used were titanium butoxide and titanium bis ammonium lactato dihydroxide. The ''smooth'' coating of titania on silica consisted of patches of titania deposited on the silica, and caused only a modest increase in the BET surface area: from 130 m^2/g for uncoated silica to 154 m^2/g after coating. The ''rough'' coating of titania on silica increased the surface area to 350 m^2/g. The higher surface area can be explained by the presence of titania particles 3 nm in diameter dispersed over the silica surface. The morphology is confirmed by TEM as well as SAXS and together, these two techniques provide unique insight into the morphology of oxide coatings. XPS shows that the titania was uniformly dispersed over the silica surface in the sample with the ''smooth'' coating and the Ti/Si ratio was consistent with the overall elemental analysis. However, on the sample with the ''rough'' coating, the XPS elemental ratio was considerably lower than the bulk elemental analysis. TEM confirms that part of the titania in this sample was present as second-phase aggregates. However, these aggregates are associated with the silica phase which helps provide excellent thermal stability even after calcination to 873 K in air. At this temperature, bulk titania prepared from the same precursor suffers a drastic loss in surface area. This work has also shown that the titania coatings can be prepared via water-soluble precursors (namely TALH) eliminating the need for solvents inherent in the use of the more reactive alkoxide precursors. These titania coatings can be used to modify support chemistry and metal–silica interactions and they can also provide tita-

nia in high surface form both as a photocatalyst and a catalyst support.

Acknowledgement

This work was supported by US Department of Energy grant number DE-FG22-95PC95210 and by the US Department of Energy, Fossil Energy Advanced Research and Technology Development Materials Program. This work was partially supported by the United States Department of Energy under contract DE-AC04-94AL85000. Sandia is a multiprogram laboratory operated by Sandia Corporation, a Lockheed Martin Company, for the United States Department of Energy. Transmission electron microscopy was performed at the electron microbeam analysis laboratory located in the department of Earth and Planetary Sciences, University of New Mexico. We thank John Hussler for assistance with the XRF and AA measurements and Paul Hubbard for assistance with the SAXS data collection. We also thank Norton Chemical Process Products Corporation for providing samples of the silica gel.

References

[1] D.F. Ollis, E. Pelizetti and N. Serpone, Environ. Sci. Technol. 25 (1991) 1523.
[2] A. Baiker, P. Dollenmeir and M. Glinski, Appl. Catal. 35 (1987) 351.
[3] S. Srinivasan, A.K. Datye, M. Hampden-Smith and C.H.F. Peden, J. Catal. 145 (1994) 565.
[4] S. Srinivasan, A.K. Datye, M. Hampden-Smith, I.E. Wachs, G. Deo, J.M. Jehng, A. Turek and C.H.F. Peden, J. Catal. 131 (1991) 260.
[5] T.T. Borek, X. Qui, L. Rafuse, A.K. Datye and R.T. Paine, J. Am. Ceram. Soc. 74 (1991) 2587.
[6] W. Stöber, A. Fink and E.J. Bohn, Colloid Interf. Sci. 26 (1968) 62.
[7] A. Hanprasopwattana, S. Srinivasan, A.G. Sault and A.K. Datye, Langmuir 12 (1996) 3173.
[8] A.I. Biaglow, R.J. Gorte, S. Srinivasan and A.K. Datye, Catal. Lett. 13 (1992) 313.
[9] A.K. Datye, S. Srinivasan, L.F. Allard, C.H.F Peden, J.R. Brenner and L.T. Thompson, J. Catal. 158 (1996) 205.
[10] O. Glatter and Kratky, *Small-Angle X-ray Scattering* (Academic Press, New York, 1982).
[11] M. Kallala, C. Sanchez and B. Cabane, J. Non-Cryst. Solids 147/148 (1992) 189.
[12] K.D. Keefer and D.W. Schaefer, in: *Fractals in Physics*, eds. L. Pietronero and E. Tosatti (Elsevier, Amsterdam, 1986) p. 39.
[13] J.M. Drake, P. Levitz and S. Sinha, Mater. Res. Soc. Symp. Proc. 73 (1986) 305.
[14] A. Fernandez, J. Leyrer, A.R. Gonzalez-Elipe, G. Munuera and H. Knözinger, J. Catal. 112 (1988) 489.
[15] S. Haukka, E-L. Lakomaa, J. Jylhä Vilhunen and S. Hornytzkyz, Langmuir 9 (1993) 3497.
[16] R. Castillo, B. Koch, P. Ruiz and B. Delmon, J. Mater. Chem. 4 (1994) 903.
[17] R. Castillo, B. Koch, P. Ruiz and B. Delmon, J. Catal. 161 (1996) 524.
[18] K. Nishiwaki, N. Kakuta, A. Ueno and H. Nakabayashi, J. Catal. 118 (1989) 498.
[19] G. Beaucage, J. Appl. Cryst. 28 (1995) 717.
[20] P.W. Schmidt, J. Appl. Cryst. 15 (1982) 567.
[21] T.A. Witten, Phys. Rev. Lett. 47 (1981) 1400.
[22] F.P.J.M. Kerkhof and J.A. Moulijn, J. Phys. Chem. 83 (1979) 1612.
[23] A. Frydman, D.G. Castner, M. Schmal and C.T. Campbell, J. Catal. 157 (1995) 133.
[24] M.P. Seah and W.A. Dench, Surf. Interf. Anal. 1 (1979) 2.
[25] C.D. Wagner, L.E. Davis, M.V. Zeller, J.A. Taylor, R.M. Raymond and L.H. Gale, Surf. Interf. Anal. 3 (1981) 211.